

# Suspended, Shrinkage-Free, Electrospun PLGA Nanofibrous Scaffold for Skin Tissue Engineering

Changhai Ru,<sup>\*,†,‡,||</sup> Feilong Wang,<sup>†</sup> Ming Pang,<sup>‡</sup> Lining Sun,<sup>†</sup> Ruihua Chen,<sup>\*,§</sup> and Yu Sun<sup>\*,†,‡,||</sup>

<sup>†</sup>Research Center of Robotics and Micro System & Collaborative Innovation Center of Suzhou NanoScience and Technology, Soochow University, Suzhou 215021, China

<sup>‡</sup>College of Automation, Harbin Engineering University, Harbin 150001, China

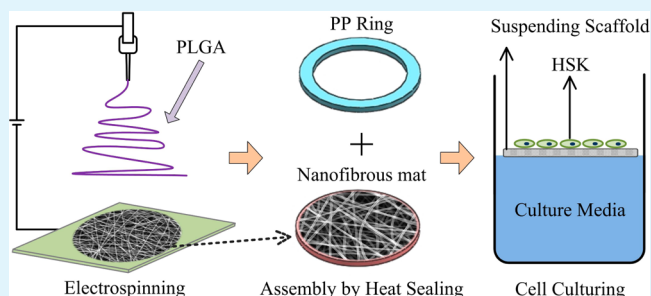
<sup>§</sup>Jiangsu Institute of Clinical Immunology, First Affiliated Hospital of Soochow University, Soochow University, Suzhou 215006, China

<sup>||</sup>Faculty of Applied Science and Engineering, University of Toronto, Toronto, Ontario M5S 3G8, Canada

## S Supporting Information

**ABSTRACT:** Electrospinning is a technique for creating continuous nanofibrous networks that can architecturally be similar to the structure of extracellular matrix (ECM). However, the shrinkage of electrospun mats is unfavorable for the triggering of cell adhesion and further growth. In this work, electrospun PLGA nanofiber assemblies are utilized to create a scaffold. Aided by a polypropylene auxiliary supporter, the scaffold is able to maintain long-term integrity without dimensional shrinkage. This scaffold is also able to suspend in cell culture medium; hence, keratinocyte cells seeded on the scaffold are exposed to air as required in skin tissue engineering. Experiments also show that human skin keratinocytes can proliferate on the scaffold and infiltrate into the scaffold.

**KEYWORDS:** electrospinning, suspending scaffold, scaffold shrinkage, skin tissue engineering, keratinocyte



## 1. INTRODUCTION

Skin represents approximately one-tenth of the body mass and is necessary for animal survival.<sup>1–3</sup> It serves several important functions, including as a physical barrier to the external environment, thermal regulation, and retention of normal hydration.<sup>4,5</sup> In the past decades, many skin substitutes, such as xenografts, autografts, and allografts, have been used to treat burns or other skin defects.<sup>6–8</sup> However, because of factors, such as immune response, these skin substitutes are not yet able to fully meet the requirements of skin recovery.<sup>9</sup> Hence, tissue engineering has been under intense development and has shown significant promise in creating skin tissue substitutes.<sup>10–13</sup>

One challenge in tissue engineering is the design of reproducible three-dimensional (3D) scaffolds that can mimic the structure and biological functions of the natural extracellular matrix (ECM), for guiding cellular migration providing mechanical support, and regulating cellular activities.<sup>14</sup> Compared to other methods for the fabrication of nanofibrous scaffolds, such as meltblowing,<sup>15</sup> drawing,<sup>16</sup> phase-separation<sup>17</sup> and self-assembly,<sup>18</sup> electrospinning is a versatile technique for producing tissue engineering scaffolds with individual fiber diameters ranging from a few nanometers to hundreds of nanometers.<sup>19,20</sup> Furthermore, it also enables the production of nanofibers from a wide variety of materials including polymers, composites, metals, oxides, semiconductors and ceramics.<sup>21</sup>

Electrospun nanofibers are structurally similar to collagen in ECM. In addition, the high surface area and highly porous structure of fibrous mats make them suitable for culturing cells and tissues. However, dimensional shrinkage and distortion of the electrospun scaffolds restrict the initial adhesion and further growth of cells.<sup>22–27</sup> For instance, PLGA electrospun scaffolds have accepted biocompatibility and biodegradability, and have excellent fiber-forming properties. However, they shrink almost by 80% when immersed in cell culture medium at 37 °C for 2 h.<sup>28</sup> The significant change in dimension and porosity is unfavorable for cells to infiltrate into the scaffold structures.<sup>29</sup>

To tackle the scaffold shrinkage issue, Jin et al. proposed the blending of PDLA and poly(ethylene glycol) (PEG) with different PEG contents to form scaffolds via electrospinning.<sup>30</sup> Although the shrinkage issue was partially overcome by tuning different blending proportions, this approach is not widely applicable to other biomaterials.<sup>31</sup> Zhou et al. reported the use of a copper grid as the collector to obtain nest-like nanofibrous PLGA scaffolds and prevent the fibers from contracting into the center part.<sup>32</sup> Compared to ~80% shrinkage in traditional PLGA scaffolds, dimensional shrinkage was still 53%. To prevent scaffold shrinkage and fiber morphology changes,

Received: March 4, 2015

Accepted: May 5, 2015

Published: May 5, 2015

fibrous scaffolds can be fixed to CellCrown plastic rings. As immobilized firmly on a rigid body, the scaffold can maintain its original structure during cell culture.<sup>33</sup> However, culture medium level must be carefully maintained to ensure that cells on the scaffold properly contact culture medium at all time, which is a time-consuming task.

In this work, widely used biodegradable polyester PLGA<sup>34–36</sup> was electrospun to form nanofibrous mats. To alleviate dimensional shrinkage, the mat was fixed onto an auxiliary ring made of polypropylene (PP) with a thickness of 0.2 mm to form a complete scaffold. Since the density of PP is lower than that of water, the scaffold floats on cell-culture medium. As a result, cells seeded on the scaffold obtain nutrients through the porous mat and are exposed to air throughout culturing. Thus, it serves as an ECM template for cell adhesion and tissue development and mimics the human epidermal tissue forming environment.

## 2. MATERIALS AND METHODS

**2.1. Materials.** Poly(lactic-co-glycolic acid, MW = 40 000) with a ratio of 50:50 was purchased from JiNan DaiGang Biomaterial Co.. Tetrahydrofuran (THF) and dimethylformamide (DMF) used as solvent were purchased from Shanghai Liming Industrial and Trade Co. Ethyl alcohol was provided by Shanghai Haohua Chemical Co.. Human skin keratinocytes and culture solution were obtained from the Institute of Clinical Immunology in the First Affiliated Hospital of Soochow University.

**2.2. Preparation of PLGA Nanofibers by Electrospinning.** An electrospinning apparatus built in house was constructed using a high voltage power supplier (Tianjindongwen, China), a syringe pump (Cole Parmer, USA), a syringe with a stainless steel blunt-ended needle (inner diameter: 110  $\mu\text{m}$ ), and a custom-made rotating mandrel-type collector (Tongliweina Nanotechnology Co., Ltd., 150–6000 rpm) (see Figure S1 in Supporting Information). PLGA solutions with concentrations of 0.2%, 0.3%, 0.4%, 0.5% (wt/vol) were prepared by dissolving block copolymer in a solvent mixture of THF and DMF with a weight ratio of 3:1 and stirred for 24 h at room temperature. The polymer solution was then loaded into a 5 mL plastic syringe and mounted on the syringe pump. For electrospinning, a stainless steel needle with an inner diameter of 0.6 mm was connected to a high voltage power supply that was operated at 15 kV. The distance between the needle tip and the collector was 20 cm. The solution was extruded out of the syringe at a constant flow rate of 0.8 mL/h.

### 2.3. Characterization of Electrospun Nanofibers.

**2.3.1. Morphology of Nanofibers.** After electrospinning, each sample was randomly cut at different locations on the electrospun nanofiber assemblies. The sample surfaces were coated with gold using a sputtering system (Sputter Coater E-1045, Hitachi, Japan) before SEM imaging (S4800, Hitachi, Japan). SEM images were analyzed by using ImageTool-3.4 to determine morphological appearance, average diameter, and orientations of electrospun nanofibers.

**2.3.2. Pore Size and Porosity of Scaffold.** Pore size and size distribution of the nanofiber assemblies were also evaluated by using ImageTool-3.4. Porosity of the electrospun nanofiber scaffolds were determined according to a method reported previously.<sup>37</sup> Briefly, rectangular samples were cut from the electrospun nanofiber structures, and their length, width and thickness were measured using a micrometer to calculate volume ( $V$ ). The weight ( $m$ ) of the samples was measured by

an analytical balance. The density ( $\rho_i$ ) of each sample was calculated from its volume ( $V_i$ ) and weight ( $m_i$ ). Porosity ( $\varepsilon$ ) was determined from the average density ( $\rho$ ) of the samples and the standard density of PLGA ( $\rho_0 = 1.145\text{g/ml}$ ) according to<sup>38</sup>

$$\varepsilon = \left(1 - \frac{\rho}{\rho_0}\right) \times 100 \quad (1)$$

## 2.4. Nanofiber Scaffolds Suspending in Culture Medium.

**2.4.1. Fabrication of Nanofiber Scaffolds.** As illustrated in Figure 1, the nanofiber assemblies after electro-

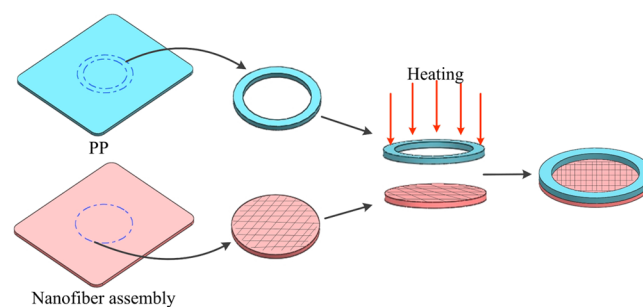


**Figure 1.** Schematic illustrating steps for constructing suspending nanofiber scaffolds.

spinning were opened longitudinally and cut into circular membranes with a diameter of 20 mm. An auxiliary plastic ring made of polypropylene (PP) paper (thickness = 0.2 mm; outer diameter = 20 mm; inner diameter = 18 mm) was heat sealed with the circular PLGA nanofiber membrane (temperature = 80  $^{\circ}\text{C}$ ; force = 0.2 N). Since the melting point of PLGA and PP are approximately 60 and 170  $^{\circ}\text{C}$  respectively, the PLGA membrane fuse onto the PP ring to form a complete scaffold.

**2.4.2. Floating Test.** The scaffolds were washed three times (2 min per time) with 70% ethanol. The scaffold was then soaked into sterilized phosphate buffered saline (pH 7.2, PBS) and incubated at 37  $^{\circ}\text{C}$ . The PBS solution was not changed throughout the 15-day floating test period.

**2.4.3. Shrinkage Evaluation.** Suspending scaffolds along with PLGA membranes (without auxiliary rings) were placed in closed containers filled with 5 mL of PBS (pH 7.4) and incubated at 37  $^{\circ}\text{C}$  for 1 day. They were subsequently freeze-dried. The area ( $S$ ) of the dried samples was measured and compared to their initial area ( $S_0$ ). The shrinkage percentage was calculated according to

$$\omega = \left(1 - \frac{S}{S_0}\right) \times 100 \quad (2)$$

**2.5. Cells and Cell Culture.** Human skin keratinocytes (HSK) were taken from human foreskins derived from donors who underwent surgery. Briefly, HSK cells were extracted from epidermis and seeded in conditional skin culture medium containing epidermal growth factors. The cells grew into colonies after 1 week. When they proliferated at approximately 70% confluency, the cells were trypsin digested for 5 min. Cells ( $1 \times 10^4$ ) were seeded on each film, and scaffolds with cells were placed in a 6-well culture plate with 2 mL of medium per well and incubated at 37  $^{\circ}\text{C}$  under 5%  $\text{CO}_2$ . Culturing medium was changed every 2 days.

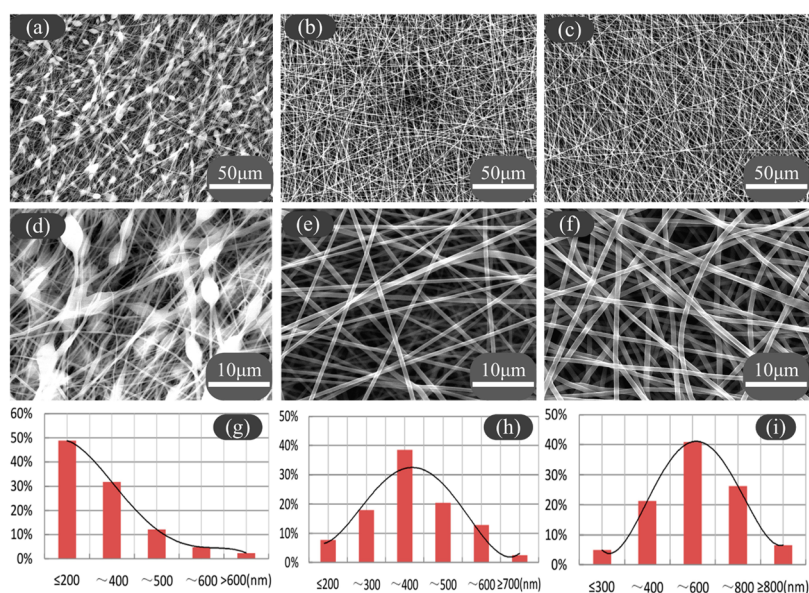


**Figure 2.** (a, d, g) Nanofibers formed when PLGA concentration of 0.2 g/mL was used. (b, e, h) Nanofibers formed when PLGA concentration of 0.3 g/mL was used. (c, f, i) Nanofibers formed when PLGA concentration of 0.4 g/mL was used.

**2.6. Characterization of Cell Behavior on Suspending Scaffolds.** SEM was used to quantify HSK morphologies on nanofiber scaffolds. Briefly, samples were harvested on days 1, 3, and 5 after seeding, washed with PBS twice to remove residual culture solution and nonattached cells, and then fixed with 4% glutaraldehyde for 2 h at 4 °C. Fixed samples were washed repeatedly with PBS to remove glutaraldehyde and then air-dried overnight. Dry cellular constructs were sputter coated with gold and imaged under SEM. Then, cell covering areas on the electrospun scaffolds were determined by measuring cell contours in SEM images.

**2.7. Statistical Analysis.** The values were expressed as means  $\pm$  standard deviation (SD). Whenever appropriate, two-tailed Student's *t* test was used to discern the statistical difference between groups. A probability value (*p*) of less than 0.05 was considered to be statistically significant.

### 3. RESULTS AND DISCUSSION

**3.1. Electrospun Nanofiber Assemblies.** The concentration of electrospinning solution played an important role to the electrospinning dynamics and nanofiber morphology. For a concentration lower than 0.3 g/mL, a high number of beads were formed (Figure 2a and d). This phenomenon is attributed to the viscosity of the solution which was too low to form fibers with uniform morphologies. When concentration was increased, spinnability of PLGA was enhanced. When PLGA concentration reached 0.3 g/mL, homogeneous fibers were formed (Figure 2b and e). When the content of PLGA was further increased, fiber uniformity became more obvious (Figure 2c and f).

In the meanwhile, the diameter of the electrospun nanofibers also increased with higher PLGA concentrations. As summarized in Figure 2g–i, for a concentration of 0.2 g/mL (Figure 2g), the mean fiber diameter was approximately 300 nm. For concentrations of 0.3 g/mL (Figure 2h) and 0.4 g/mL (Figure 2i), the average fiber diameters were 400 and 600 nm, respectively. When the concentration reached a critical value (0.5 g/mL in our experiments), surface tension became too strong to overcome, and no PLGA nanofibers formed.

### 3.2. Pore Size and Porosity of Nanofiber Assemblies.

Nanofibrous scaffolds used for tissue engineering including skin reconstitution should be made porous for cells to infiltrate into the scaffold and proliferate. The porous structure is also required for ensuring sufficient gas and nutrient exchange for tissue regeneration.<sup>39</sup> Structural pore properties were assessed for the electrospinning-constructed scaffolds with different PLGA concentrations. The very fine nanofibers form highly porous assemblies, providing large surface areas and space for cell adhesion and migration. As summarized in Table 1, the

**Table 1. Characteristics of Electrospun Nanofiber Assemblies**

concentration (g/mL)	pore size ( $\mu\text{m}$ )	porosity (%)
0.2	$3 \pm 0.2$	20
0.3	$8 \pm 0.5$	72
0.4	$7 \pm 0.3$	78

average pore size of the PLGA nanofibrous assemblies with 0.2 g/mL concentration was 3  $\mu\text{m}$ . Larger pore sizes were obtained at higher PLGA concentrations. At the concentration of 0.3 g/mL, average pore size of the nanofibrous assembly reached 8  $\mu\text{m}$ .

Scaffold porosity suitable for cellular penetration is typically in the range of 60–90%.<sup>40</sup> Thus, we selected the electrospun nanofibrous assemblies with a PLGA concentration of 0.3 g/mL for cell experiments. Within this scaffold porosity range, average pore sizes differed significantly in previous studies, ranging from 5–15<sup>10</sup> to 132.7  $\mu\text{m}$ <sup>14</sup> for fibroblast growth. The average pore sizes of our electrospun scaffolds for HSK cell growth were 8  $\mu\text{m}$ ; however, the optimized selection of pore sizes requires further investigation.

**3.3. Shrinkage Behavior.** During electrospinning, polymer solution is subjected to a high electric field. This process results in a high degree of alignment and orientation of polymer chains in the nanofiber assembly but also induces inner stress.<sup>30</sup> When immersed into solvent at a temperature higher than 35 °C, macromolecular chains can rapidly relax, which undesirably

causes dimensional shrinkage of the PLGA fibrous assembly. Figure 3a and b shows an original and shrunken fibrous

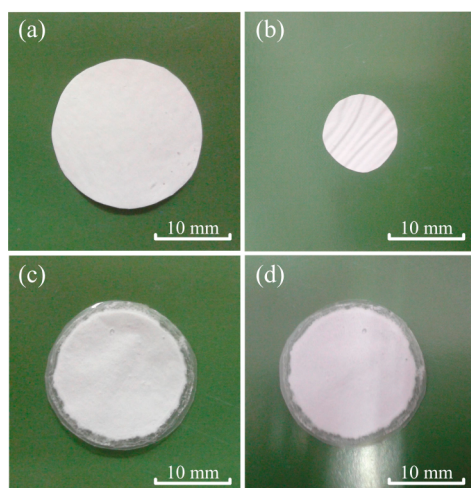


**Figure 3.** Shrinkage test of fibrous membranes. (a, b) Nanofibrous assembly before and after incubation in PBS at 37 °C for 24 h. (c) Scaffold formed by fusing a nanofibrous assembly on a PP ring. (d) The same scaffold after incubation in PBS at 37 °C for 24 h.

assembly after incubating in PBS at 37 °C for 24 h. Shrinkage from its initial size was more than 75%. Similar shrinkage behavior was also reported in other studies.<sup>28</sup> In contrast, for a PLGA scaffold consisting of a nanofiber assembly fused on a PP ring, no observable shrinkage occurred because of the enhanced mechanical property. Figure 3c and d shows an original scaffold and the same scaffold after incubation in PBS at 37 °C for 24 h.

**3.4. Suspended Scaffolds.** Polypropylene (PP) is mechanically strong, chemically stable, and biocompatible. It has a density of 0.91 g/cm<sup>3</sup> enabling the scaffold to suspend in cell culture medium. The use of a PP ring as auxiliary support serves two purposes: (1) to make the overall nanofiber scaffold suspend in liquid, which is necessary for skin cells to be exposed to air during growth, and (2) to prevent nanofiber assemblies from shrinking and maintain long-term membrane integrity. In our experiments, the fibrous membrane was initially suspended on PBS surface (see Figure S2 in Supporting Information). However, the membrane sunk to the bottom of the beaker after a few hours due to dimensional shrinkage and increased density. For scaffolds consisting of nanofiber assemblies fused on a PP ring, the scaffold remained suspended on PBS surface throughout the 15-day testing period.

**3.5. Cell Growth on PLGA Nanofiber Scaffolds.** Cell morphology on the PLGA scaffolds was studied via SEM imaging (see Figure S3 in Supporting Information). Figure 4a and b shows HSK growth on a representative nanofibrous scaffold at day 1 and day 5. The scaffold was formed with a PLGA concentration of 0.3 g/mL. As summarized in Figure 4c, HSKs only reached a confluency of approximately 8% at day 1. This was because of the low HSK seeding density used in this work in order to observe cell proliferation over a 5-day period. At days 3 and 5, the confluency of HSKs increased to 22% and to 53%, respectively.

In this process, it was observed that there were cells infiltrating into the nanofibrous assembly, and the cells gradually join to cover the scaffold surface. To investigate the behavior of cell infiltration into the nanofibrous scaffold, hematoxylin, and eosin staining was conducted and cross sections were prepared. Figure 4d shows typical HSK cell

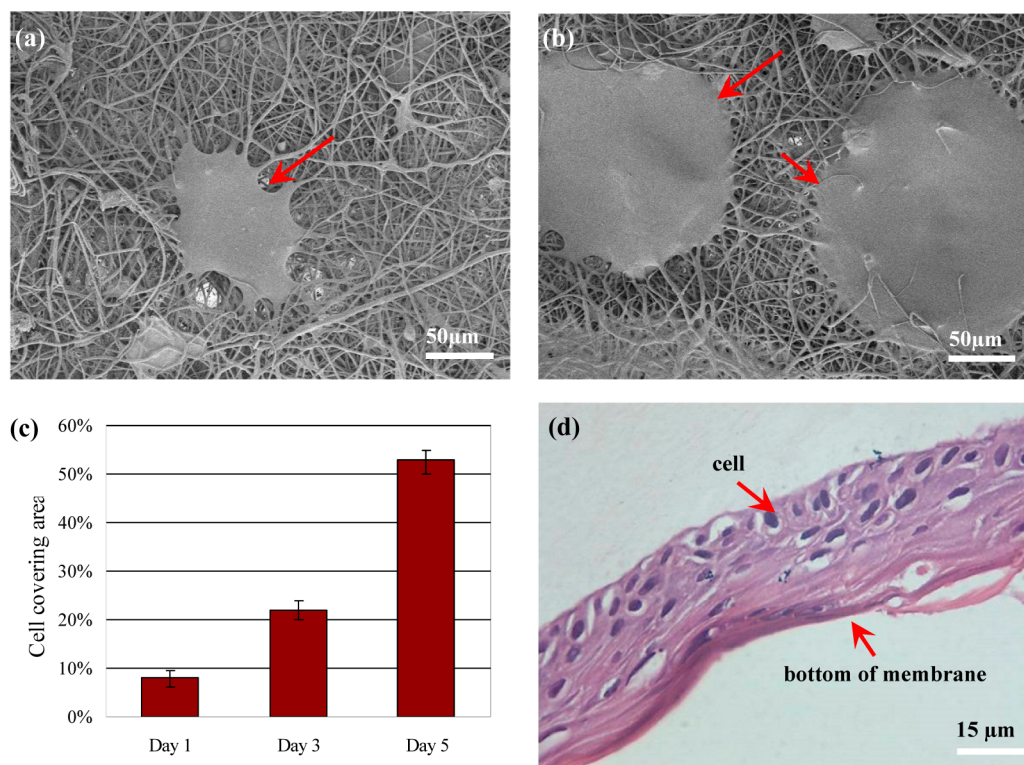


**Figure 4.** SEM images of HSK cells grown on PLGA scaffold after incubation for (a) 1 and (b) 5 days. Arrows indicate HSK cells. (c) Cell covering area over 5-day growth period. (d) Cross section of the scaffold with cells infiltrating into the fibrous mats.

penetration into the scaffold and their distributions inside the fibrous scaffold. During cell growth, the suspending PLGA scaffolds provided a three-dimensional nanofibrous host environment for skin cells to adhere, infiltrate, and proliferate.

#### 4. CONCLUSION

Skin tissue engineering scaffolds were constructed by electrospinning of PLGA nanofibers. With the auxiliary support from a polypropylene (PP) ring, the electrospun PLGA mat is able to maintain its initial shape and size without drastic dimensional shrinkage in cell culture medium. The scaffold is also able to stay suspended on the surface of cell culture medium, necessary for skin cells to be exposed to air during growth to form human epidermal tissue. Nanofiber sizes and scaffold porosities with different PLGA concentrations were quantified. Human skin keratinocytes were cultured on the scaffold. Cell proliferation and infiltration were observed.

#### ■ ASSOCIATED CONTENT

##### ● Supporting Information

Experimental setup, suspension of scaffolds, and calculation of cell distribution percentage. The Supporting Information is available free of charge on the ACS Publications website at DOI: 10.1021/acsami.5b01953.

#### ■ AUTHOR INFORMATION

##### Corresponding Authors

\*E-mail: rzh@suda.edu.cn.

\*E-mail: hsy139@126.com.

\*E-mail: sun@mie.utoronto.ca.

##### Notes

The authors declare no competing financial interest.

#### ■ ACKNOWLEDGMENTS

Authors acknowledge financial support from the Instrument Development Major Program of National Natural Science Foundation of China (Grant No. 61327811), National Natural Science Foundation of China (Grant No. 61174087), Jiangsu Natural Science Funds for Distinguished Young Scholar (Grant No. BK2012005), Shanghai Municipal Science and Technology Commission Project (Grant No. 14JC1491500), and the Canada Research Chairs Program.

#### ■ REFERENCES

- (1) Mansbridge, J. Skin Tissue Engineering. *J. Biomater. Sci., Polym. Ed.* **2008**, *19*, 955–968.
- (2) Marino, D.; Reichmann, E.; Meuli, M. Skingineering. *Eur. J. Pediatr. Surg.* **2014**, *24*, 205–213.
- (3) Chandrasekaran, A. R.; Venugopal, J.; Sundarajan, S.; Ramakrishna, S. Fabrication of a Nanofibrous Scaffold with Improved Bioactivity for Culture of Human Dermal Fibroblasts for Skin Regeneration. *Biomed. Mater.* **2011**, *6*, 015001.
- (4) Chong, E. J.; Phan, T. T.; Lim, I. J.; Zhang, Y. Z.; Bay, B. H.; Ramakrishna, S.; Lim, C. T. Evaluation of Electrospun PCL/Gelatin Nanofibrous Scaffold for Wound Healing and Layered Dermal Reconstitution. *Acta Biomater.* **2007**, *3*, 321–330.
- (5) Kumbar, S. G.; Nukavarapu, S. P.; James, R.; Nair, L. S.; Laurencin, C. T. Electrospun Poly(Lactic Acid-co-glycolic Acid) Scaffolds for Skin Tissue Engineering. *Biomaterials* **2008**, *29*, 4100–4107.
- (6) Hemmerling, J.; Wegner, K. J.; Stebut, E.; Wolff, D.; Wagner, E. M.; Hartwig, U. F.; Meyer, R. G. Human Epidermal Langerhans Cells Replenish Skin Xenografts and are Depleted by Alloreactive T Cells in Vivo. *J. Immunol.* **2011**, *187*, 1142–1149.
- (7) Cirodde, A.; Leclerc, T.; Jault, P.; Duhamel, P.; Lataillade, J. J.; Bargaes, L. Cultured Epithelial Autografts in Massive Burns: A Single-Center Retrospective Study with 63 Patients. *Burns* **2011**, *37*, 964–972.
- (8) Catalano, E.; Cochis, A.; Varoni, E.; Rimondini, L.; Azzimonti, B. Tissue-Engineered Skin Substitutes: An Overview. *J. Artif. Organs* **2013**, *16*, 397–403.
- (9) Chen, H.; Huang, J.; Yu, J.; Liu, S.; Gu, P. Electrospun Chitosan-graft-poly( $\epsilon$ -caprolactone)/Poly( $\epsilon$ -caprolactone) Cationic Nanofibrous Mats as Potential Scaffolds for Skin Tissue Engineering. *Int. J. Biol. Macromol.* **2011**, *48*, 13–19.
- (10) Yang, S.; Leong, K. F.; Du, Z.; Chua, C. K. The Design of Scaffolds for Use in Tissue Engineering. Part I. Traditional factors. *Tissue Eng.* **2001**, *7*, 679–689.
- (11) Jana, B.; Zeisberger, S. M.; Hoerstrup, S. P. Prenatally Harvested Cells for Cardiovascular Tissue Engineering: Fabrication of Autologous Implants Prior to Birth. *Placenta* **2011**, *32*, S316–S319.
- (12) Biedermann, T.; Boettcher, H. S.; Reichmann, E. Tissue Engineering of Skin for Wound Coverage. *Eur. J. Pediatr. Surg.* **2013**, *23*, 375–382.
- (13) Jana, S.; Tefft, B. J.; Spoon, D. B.; Simari, R. D. Scaffolds for Tissue Engineering of Cardiac Valves. *Acta Biomater.* **2014**, *10*, 2877–2893.
- (14) Zhu, X.; Cui, W.; Li, X.; Jin, Y. Electrospun Fibrous Mats with High Porosity as Potential Scaffolds for Skin Tissue Engineering. *Biomacromolecules* **2008**, *9*, 1795–1801.
- (15) Ellison, C. J.; Phatak, A.; Giles, D. W.; Macosko, C. W.; Bates, F. S. Melt Blown Nanofibers: Fiber Diameter Distributions and Onset of Fiber Breakup. *Polymer* **2007**, *48*, 3306–3316.
- (16) Nain, A. S.; Wong, J. C.; Amon, C.; Sitti, M. Drawing Suspended Polymer Micro-/Nanofibers Using Glass Micropipettes. *Appl. Phys. Lett.* **2006**, *89*, No. 183105.
- (17) Liu, X.; Ma, P. X. Phase Separation, Pore Structure, and Properties of Nanofibrous Gelatin Scaffolds. *Biomaterials* **2009**, *30*, 4094–4103.
- (18) Gao, Y.; Kuang, Y.; Guo, Z. F.; Krauss, I. J.; Xu, B. Enzyme-Instructed Molecular Self-Assembly Confers Nanofibers and A Supramolecular Hydrogel of Taxol Derivative. *J. Am. Chem. Soc.* **2009**, *131*, 13576–13577.
- (19) Frenot, A.; Chronakis, I. S. Polymer Nanofibers Assembled by Electrospinning. *Curr. Opin. Colloid Interface Sci.* **2003**, *8*, 64–75.
- (20) Greiner, A.; Wendorff, J. H. Electrospinning: A Fascinating Method for the Preparation of Ultrathin Fibers. *Angew. Chem., Int. Ed.* **2007**, *46*, 5670–5703.
- (21) Huang, Z. M.; Zhang, Y. Z.; Kotaki, M.; Ramakrishna, S. A Review on Polymer Nanofibers by Electrospinning and Their Applications in Nanocomposites. *Compos. Sci. Technol.* **2003**, *63*, 2223–2253.
- (22) Cui, W.; Cheng, L.; Li, H.; Zhou, Y.; Zhang, Y. G.; Chang, J. Preparation of Hydrophilic Poly(L-Lactide) Electrospun Fibrous Scaffolds Modified with Chitosan for Enhanced Cell Biocompatibility. *Polymer* **2012**, *53*, 2298–2305.
- (23) Xie, Z.; Buschle, D. G.; DeInnocentes, P.; Bird, R. C. Electrospun Poly(D,L)-Lactide Nonwoven Mats for Biomedical Application: Surface Area Shrinkage and Surface Entrapment. *J. Appl. Polym. Sci.* **2011**, *122*, 1219–1225.
- (24) Meng, L.; Arnoult, O.; Smith, M.; Wnek, G. E. Electrospinning of In Situ Crosslinked Collagen Nanofibers. *J. Mater. Chem.* **2012**, *22*, 19412–19417.
- (25) Torbati, A. H.; Mather, R. T.; Reeder, J. E.; Mather, P. T. Fabrication of A Light-Emitting Shape Memory Polymeric Web Containing Indocyanine Green. *J. Biomed. Mater. Res., Part B* **2014**, *102*, 1236–1243.
- (26) Li, K.; Mao, B.; Cebe, P. Electrospun Fibers of Poly(Ethylene Terephthalate) Blended with Poly(Lactic Acid). *J. Therm. Anal. Calorim.* **2014**, *116*, 1351–1359.
- (27) Terai, H.; Hannouche, D.; Ochoa, E.; Yamano, Y.; Vacanti, J. P. In Vitro Engineering of Bone Using A Rotational Oxygen-Permeable Bioreactor System. *Mater. Sci. Eng.: C* **2002**, *20*, 3–8.

- (28) Liu, Y. J.; Jiang, H. L.; Li, Y.; Zhu, K. J. Control of Dimensional Stability and Degradation Rate in Electrospun Composite Scaffolds Composed of Poly(D,L-Lactide-co-glycolide) and Poly( $\epsilon$ -Caprolactone). *Chin. J. Polym. Sci.* **2008**, *26*, 63–71.
- (29) Cui, W.; Li, X.; Zhou, S.; Weng, J. Degradation Patterns and Surface Wettability of Electrospun Fibrous Mats. *Polym. Degrad. Stab.* **2008**, *93*, 731–738.
- (30) Cui, W.; Zhu, X.; Yang, Y.; Li, X.; Jin, Y. Evaluation of Electrospun Fibrous Scaffolds of Poly(DL-Lactide) and Poly(Ethylene Glycol) for Skin Tissue Engineering. *Mater. Sci. Eng.: C* **2009**, *29*, 1869–1876.
- (31) Hiep, N. T.; Lee, B. T. Electro-Spinning of PLGA/PCL Blends for Tissue Engineering and Their Biocompatibility. *J. Mater. Sci.: Mater. Med.* **2010**, *21*, 1969–1978.
- (32) Zhou, X.; Cai, Q.; Yan, N.; Deng, X.; Yang, X. In Vitro Hydrolytic and Enzymatic Degradation of Nestlike-Patterned Electrospun Poly (D,L-lactide-co-glycolide) Scaffolds. *J. Biomed. Mater. Res., Part A* **2010**, *95*, 755–765.
- (33) Gualandi, C.; Govoni, M.; Foroni, L.; Valente, S.; Bianchif, M.; Giordano, E.; Pasquinelli, G.; Biscarini, F.; Focarete, M. L. Ethanol Disinfection Affects Physical Properties and Cell Response of Electrospun Poly(L-Lactic Acid) Scaffolds. *Eur. Polym. J.* **2012**, *48*, 2008–2018.
- (34) Leung, L.; Chan, C.; Baek, S.; Naguib, H. Comparison of Morphology and Mechanical Properties of PLGA Bioscaffolds. *Biomed. Mater.* **2008**, *3*, No. 025006.
- (35) Baker, S. C.; Rohman, G.; Southgate, J.; Cameron, N. R. The Relationship Between the Mechanical Properties and Cell Behaviour on PLGA and PCL Scaffolds for Bladder Tissue Engineering. *Biomaterials* **2009**, *30*, 1321–1328.
- (36) Anderson, J. M.; Shive, M. S. Biodegradation and Biocompatibility of PLA and PLGA Microspheres. *Adv. Drug Delivery Rev.* **2012**, *64*, 72–82.
- (37) Ru, C. H.; Wang, F. L.; Ge, C. C.; Luo, J. Note: A Multifunctional Electrospinning System for Manufacturing Diversified Nanofibrous Structures. *Rev. Sci. Instrum.* **2014**, *84*, No. 086107.
- (38) Wang, F. L.; Zhang, W. B.; Shao, Z. S.; Sun, Y.; Ru, C. H. Electrospinning System with Tunable Collector for Fabricating Three-Dimensional Nanofibrous Structures. *Micro Nano Lett.* **2014**, *9*, 24–27.
- (39) Naghibzadeh, M. Nanofibers for Skin Regeneration. *Trends Biomater. Artif. Organs* **2012**, *26*, 86–102.
- (40) Liu, H.; Wang, S.; Qi, N. Controllable Structure, Properties, and Degradation of the Electrospun PLGA/PLA-Blended Nanofibrous Scaffolds. *J. Appl. Polym. Sci.* **2012**, *125*, E468–E476.